J Mater Sci (2016) 51:739–747
DOI 10.1007/s10853-015-9396-z

Synthesis and characterization of highly ordered self-assembled bioactive fulleropeptides

Mira Bjelaković[1] · Tatjana Kop[1] · Veselin Maslak[2] · Dragana Milić[2]

Received: 25 May 2015 / Accepted: 28 August 2015 / Published online: 8 September 2015

Abstract A series of *N*-substituted fulleropyrrolidines containing peptide side chain was synthesized by the quantitative, TFA-mediated deprotection of the corresponding *tert*-butyl esters. The structures of all compounds were determined by comparative analysis of spectroscopic and spectrometric data. The electrochemical characterization, conducted by cyclic voltammetry at room temperature confirmed slightly attenuated reducibility in comparison to pristine C_{60} and a weak long-range electron-accepting effect of the Gly_3-fragment. The introduction of the peptide subunit led to improved solubility and enabled examination of the antioxidant properties in water environment. A notable radical scavenging activity of the fullerene subunit remained almost unchanged in all compounds. The investigation of the supramolecular self-assembling, performed by the scanning electron microscopy revealed an influence of the side chain, particularly the fraction of the hydrophobic residue, as well as the substrate structure on the final morphology. Most of the compounds underwent highly ordered multi-stage hierarchical assembling to the attractive, flower-shaped supramolecular aggregates during both the precipitation and slow evaporation of the solvent.

Electronic supplementary material The online version of this article (doi:10.1007/s10853-015-9396-z) contains supplementary material, which is available to authorized users.

✉ Dragana Milić
dmilic@chem.bg.ac.rs

Mira Bjelaković
mbjelak@chem.bg.ac.rs

Tatjana Kop
tanjakop@chem.bg.ac.rs

Veselin Maslak
vmaslak@chem.bg.ac.rs

[1] ICTM-Center for Chemistry, Belgrade, Serbia

[2] Faculty of Chemistry University of Belgrade, Belgrade, Serbia

Introduction

The unique structure of fullerenes has drawn considerable attention to diverse scientific fields ranging from material sciences [1–5] to medicinal [5–9] and supramolecular chemistry [10–13]. The conjugation of fullerene to other chemically or biologically relevant molecules, tailored size, shape, hydrophobicity, and stereo-electronic properties of obtained molecular hybrids enabled their broad biological applications. Fullerene derivatives induced enzymatic inhibition [6] and DNA photocleavage [6], expressed an antiviral [6, 7], antimicrobial [6], antiapoptotic [6], neuroprotective [6], and antioxidant [6–9] activity. Such compounds were also used in the photodynamic therapy [6], targeted imaging [6–8], drug [7, 8], and gene delivery [7]. In addition, potent ROS-scavenging capacity of fullerene derivatives encapsulated in liposomes made them suitable active compounds in cosmetics for the human skin aging deceleration [14]. Self-assembled fullerene-based clusters attracted attention not only from the supramolecular point of view but also from the applicable aspect since the level of aggregation played an important role in the manifestation of the antioxidant effect [15]. Consequently, tuning the non-covalent interactions by the alteration of the molecular structure, as well as by external stimuli [16, 17] led to the formation of different well-defined nanostructures such as spheres [18], tubes [19], vesicles [20], rods [20], wires [21], and fibers [22].

Amino acids and peptides are the most basic and essential building units for all living organisms. The

incorporation of fullerene into peptides, started more than 20 years ago with the methanofullerene pentapeptide synthesis [23], was further developed using either solution- [24–26] or solid-phase conditions [27–29]. The introduction of the carbon sphere substantially modified the original properties of amino acids and peptides, affording compounds of particular interest in structural as well as biological studies [30–34]. It has been shown that fullerene-containing amino acids and peptides inhibit the peptidase activity of HIV-1 protease [30], activate enzymes involved in the oxidative deamination of biogenic amines [31], express antigenic properties [25], exhibit the skin penetrating ability [32] even in the case where the parent peptides show no such uptake [33]. Low-lying lowest unoccupied molecular orbital of fullerene subunit can easily take up an electron, and scavenge free radical species resulting in the antioxidant activity comparable to standard antioxidant agents vitamin C [35] and Trolox [27]. The investigation of fulleropeptides is noteworthy also from the aspect of supramolecular chemistry due to the possibility of their both subunits to reassemble and form well ordered hierarchical architectures. The C_{60} cage showed a strong aggregation tendency driven by hydrophobicity and π–π stacking forces, while numerous peptide molecules demonstrated the ability to form ordered structures at the nano-scale [36]. The cryo-TEM experiments confirmed the formation of spherical and ellipsoidal supramolecular clusters of fullerene-based amino acids and peptides in aqueous solution, such revealing a significant effect of the carbon cage on the compounds self-assembling properties, as well as on the secondary structure of their peptide subunit [27]. Similar forms were detected during the SEM investigations [37, 38]—oval associates with the hydrophilic moieties directed to the surface were observed in aqueous solution, while in organic medium mainly spherical particles were formed. Their final morphology resulted from the influence of both hydrophilic and hydrophobic segments, as well as from the organic solvent properties.

In the previous work [9] we described the efficient synthesis of a good synthetic intermediate, the fulleropyrrolidinic acid **1** (Fp-GABA-OH) containing γ-aminobutyric (GABA) fragment. Its further transformations provided steroidal esters with pronounced antioxidant activity [9], fullerene-based peptides (obtained in the form of the C-protected *t*Bu esters) [39], as well as two more complex fulleropeptides functionalized with a lipophilic steroidal fragment [40]. With a suitable precursor in hand, it seemed reasonable to examine properties of hybrids consisting of two remarkably different subunits such as the highly hydrophobic fullerene core and a quite polar peptide chain. Furthermore, continuing the studies of a development of fullerene-based bioactive compounds, here we present the synthesis and characterization of fulleropeptidic acids **2**–**12** (Fig. 1). Their non-peptidic precursor, fullerene acid Fp-GABA-OH **1** was used as a reference compound in the examination of the self-assembling, electrochemical, and in vitro antioxidant properties.

Experimental

Materials

All reagents and solvents were used as purchased from Merck, Acros, Aldrich, and Fisher. Reactions were monitored by TLC on Merck silica gel 60 F_{254}-precoated plates.

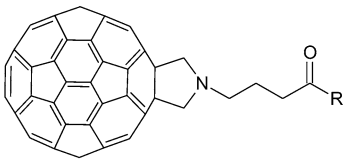

1: (Fp-GABA-OH) R = OH

2: (Fp-GABA$_2$-OH) R = HN$(CH_2)_3CO_2H$

3: (Fp-GABA$_3$-OH) R = HN$(CH_2)_3$N(H)C(=O)$(CH_2)_3CO_2H$

4: (Fp-GABA-Gly-OH) R = HNCH$_2$CO$_2$H

5: (Fp-GABA-Gly$_2$-OH) R = HNCH$_2$C(=O)NHCH$_2$CO$_2$H

6: (Fp-GABA-Gly$_3$-OH) R = HNCH$_2$C(=O)NHCH$_2$C(=O)NHCH$_2$CO$_2$H

7: (Fp-GABA$_2$-Gly-OH) R = HN$(CH_2)_3$C(=O)NHCH$_2$CO$_2$H

8: (Fp-GABA$_2$-Gly$_2$-OH) R = HN$(CH_2)_3$C(=O)NHCH$_2$C(=O)NHCH$_2$CO$_2$H

9: (Fp-GABA$_2$-Gly$_3$-OH) R = HN$(CH_2)_3$C(=O)NHCH$_2$C(=O)NHCH$_2$C(=O)NHCH$_2$CO$_2$H

10: (Fp-GABA$_3$-Gly-OH) R = HN$(CH_2)_3$C(=O)N(H)$(CH_2)_3$C(=O)NHCH$_2$CO$_2$H

11: (Fp-GABA$_3$-Gly$_2$-OH) R = HN$(CH_2)_3$C(=O)N(H)$(CH_2)_3$C(=O)NHCH$_2$C(=O)NHCH$_2$CO$_2$H

12: (Fp-GABA$_3$-Gly$_3$-OH) R = HN$(CH_2)_3$C(=O)N(H)$(CH_2)_3$C(=O)NHCH$_2$C(=O)NHCH$_2$C(=O)NHCH$_2$CO$_2$H

Fig. 1 The structures of investigated fullero-derivatives **1**–**12**

The 10 × 10 mm plates of the silicon wafer, common Al foil, and microscopic laboratory glass were used as substrates for the SEM experiments (all of them suitable for the application of both solids and solutions).

Apparatus and methods

IR spectra (ATR) were recorded on a Perkin-Elmer-FT-IR 1725X spectrophotometer and ν values are given in cm^{-1}. ^{1}H and ^{13}C NMR spectra were obtained using a Bruker Avance spectrometer at 500 and 125 MHz, respectively. The homonuclear 2D spectra (DQF-COSY, TOCSY) and the heteronuclear 2D ^{1}H–^{13}C spectra (HSQC and HMBC) were recorded with the usual settings. Samples were dissolved in the solvent system as indicated in the electronic supporting material (ESM), and tetramethylsilane (TMS) was used as an internal reference. Chemical shifts (δ) are expressed in ppm relative to that of TMS and coupling constants (J) in Hz. UV spectra were recorded on a GBC-Cintra 40 UV–Vis spectrophotometer, and the HRMS spectra on an Agilent 6210 LC ESI–MS TOF spectrometer. Investigations of sample morphology were carried out with scanning electron microscopy, using a JEOL JSM-840A instrument, at an acceleration voltage of 30 kV and JFC 1100 gold ion sputter device. The antioxidant capacity of fullerosomes (fullerene acids **1–12** encapsulated liposomes) was determined by the Ferrous ion oxidation–xylenol orange (FOX) assay, according to the published procedure [41]. A detailed explanation of the FOX reagent, standard, blank, and fullerosome probes preparation is given in ESM. The electrochemical measurements were carried out on a CHI760b Electrochemical Workstation potentiostat (CH Instruments, Austin, TX, USA) using a conventional three-electrode cell (1 cm^3) equipped with a glassy carbon and Ag/Ag^+ electrode [a silver wire in contact with 0.01 M $AgNO_3$ and 0.10 M tetrabutylammonium perchlorate (TBAP)] and the platinum wire as the working, reference, and auxiliary electrodes, respectively, calibrated with a ferrocene/ferrocenyl couple (Fc/Fc^+) as an internal standard. All experiments were performed at room temperature in the potential range of −2.0 to 0.5 V versus saturated calomel electrode, at sweep rates between 0.1 and 1 Vs^{-1}.

Sample preparation

Synthesis

The model compound **1** was prepared according to the literature procedure [9], while the acids **2–12** were obtained following the general procedure for *tert*-butyl esters deprotection in the acidic media. A solution of the corresponding fulleropeptide *tert*-butyl ester [39] (0.13 mmol) in trifluoroacetic acid/dichloromethane mixture (1/1, 4 mL) was stirred at room temperature for 2 h and evaporated to dryness. An excess of the acid was removed by co-evaporation with toluene (3 × 20 mL) and the product was precipitated by adding methanol to the highly concentrated solution in dichloromethane/CS_2. After drying under reduced pressure all fulleropeptide acids were obtained as brown powders in almost quantitative yield (98–100 %). Detailed spectral data of all compounds, their spectra (IR, ^{1}H, and ^{13}C NMR, UV), and cyclic voltammograms, as well as the table containing a comparative overview of the chemical shifts of the peptide moieties are given in ESM.

SEM

The samples for investigation of the size and morphology of self-organized structures formed in solution were prepared at room temperature by 'drop drying' method [12]. The 10 μL of 1 mM solution of compounds **1–12** in PhMe/MeOH (5/1, v/v) were deposited on the substrate surface and left overnight to slowly evaporate in a covered glass petri dish (diameter 10 cm) under PhMe atmosphere. In the case of the solid samples, a small amount of the powdered tested compound was sprinkled on the substrate. All probes were gold sputtered and then subjected to the SEM observations.

Cyclic voltammetry

The electrochemical properties of fulleroacids **1–12** were investigated under inert atmosphere (argon) using their 1 mM solution in dry dimethylformamide (DMF) containing 0.1 M TBAP as a supporting electrolyte.

Fullerosome preparation [41]

The fullerene C_{60} or the fullerene acids **1–12** (0.1 mg) and fourfold mass of lecithin (0.4 mg) were dissolved in toluene (4.0 mL), and ultrasonicated for 1 min. Solvent was later removed by rotary vacuum evaporation. Lipid film was then diluted with deionized H_2O (5.0 mL) to a concentration of fullerene component of 0.02 mg/mL by gentle vortex mixing.

Antioxidant activity

The fullerosomes and vitamin C solutions, containing 0.002 mg/mL of pure compounds, were incubated with the same volume of 200 μM TBHP. The same volumes (0.050 mL) of the sample (0.02 mg/mL) and 2 mM TBHP were dissolved in 0.9 ml of H_2O and incubated at room temperature for 10 min. The FOX reagent (0.950 mL) was added to 0.050 mL of each sample, followed by 80 min

incubation at room temperature. After incubation, the absorbance at 560 nm was measured spectrophotometrically.

Results and discussion

Synthesis and structure determination

Fulleropyrrolidinic acid **1** (Fp-GABA-OH) was prepared according to the literature procedure [9], while fulleropeptides **2**–**12** were obtained quantitatively by TFA-mediated deprotection of previously synthesized fulleropeptide *t*Bu esters [39].

The structures of fulleropeptide acids were deduced by means of the HRMS, IR, UV–Vis, 1D, and 2D NMR (COSY, TOCSY, HSQC, HMBC). The most complex structure (compound **12**) is chosen as a representative of synthesized compounds and its IR, UV, ^{1}H, and ^{13}C NMR spectra are presented in Figs. 2, 3, 4, and 5, respectively, while the same images of all other fulleroacids **1**–**11** are collected in ESM. All 11 new compounds gave correct positive ESI quasimolecular $[M+1]^+$ ion peak in ESI-TOF–MS spectra and expected vibrations in the IR spectra—very broad overlapped bands of the amide NH and carboxylic OH groups in the region of 3500–3000 cm^{-1} and strong peaks of carbonyl stretching vibrations in the 1750–1600 cm^{-1} range (Fig. 2 and ESM). As their *t*Bu esters [39], all acids also displayed almost identical absorption behavior in the UV–Vis range: peaks assignable to the fulleropyrrolidine segment were observed at 254–259 and 430 nm (strong and weak sharp, respectively), while absorptions belonging to the amide region appeared in the range of ~305 and 320 nm (Fig. 3 and ESM).

^{1}H NMR spectra of all fulleropeptides (Fig. 4 and ESM) showed broad triplets at δ 7.5–8.2 ppm, singlet at δ 4.5–4.7 ppm, and doublets at δ 3.8–4 ppm, attributable to exchangeable amide, pyrrolidinic, and glycine CH_2 protons, respectively. The GABA methylene protons were established from the TOCSY cross-peaks between amide protons and CH_2 triplets at δ 2.1–2.7 ppm ($H_2C(2)$), quintets at δ 1.8–2.3 ppm ($H_2C(3)$), and triplets or quartets at δ 3.2–3.4 ppm ($H_2C(4)$).

Their ^{13}C NMR spectra (Fig. 5 and ESM) contained all peaks belonging to both fulleropyrrolidine and peptide carbons. The C_{2v} symmetric fulleropeptides exhibited 16 well-resolved lines for 58 sp^2-C atoms in a broad region of δ 135–155 ppm, as well as 2 sp^3-C peaks for fullerene C(1) and C(9) in the aliphatic region (δ ~70 ppm), together with pyrrolidinic CH_2 carbons (δ ~67 ppm).

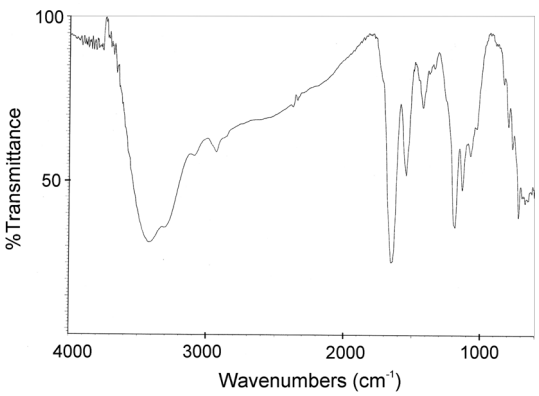

Fig. 2 IR spectrum of fulleropeptide acid **12**

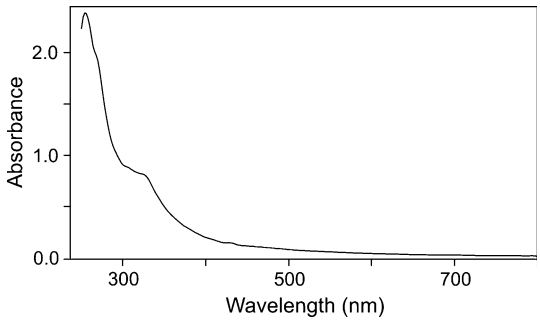

Fig. 3 UV-vis spectrum of fulleropeptide acid **12**

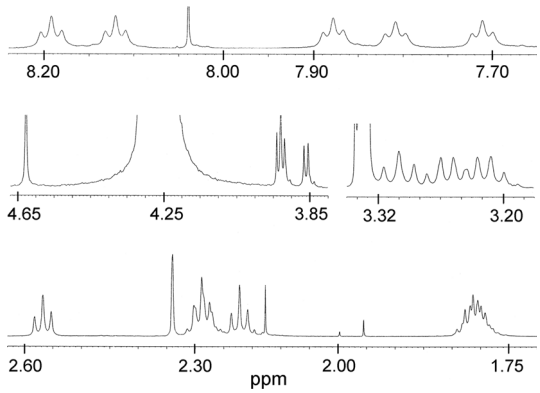

Fig. 4 Expanded parts of ^{1}H NMR spectrum of fulleropeptide acid **12**

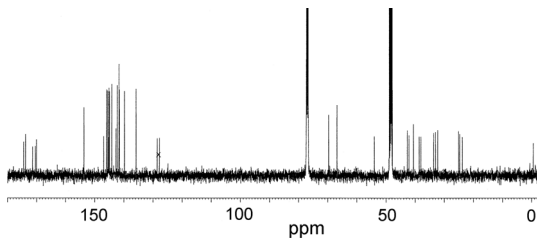

Fig. 5 ^{13}C NMR spectrum of fulleropeptide acid **12**

The ^{13}C chemical shifts of a peptidic moiety of all compounds were observed in a very narrow range: Gly CH_2 signals appeared in the region of δ 40–43, those belonging to GABA-C(2) and C(3) at δ 31–34 and 23–25 ppm, respectively. GABA-C(4) carbons, adjacent to the fulleropyrrolidine ring resonated at $\delta \sim 54$ ppm, while those next to the amide nitrogen at δ 38–39 ppm. All carbonyl carbons appeared in the expected downfield area: amides at $\delta \sim 170$ and ~ 174 ppm (Gly and GABA, respectively), and carboxylic at δ 171–172 and ~ 176 (Gly and GABA, respectively). The very narrow range of assignments of spin active nuclei of all fullerene acids and the distinctive trends found in their NMR data were largely comparable to parent *t*-Bu esters [39]. Complete and unambiguous ^{1}H and ^{13}C assignments of all spin active nuclei from peptide chains (see Table S1 ESM) could facilitate further studies, since obtained compounds represent potential bioactive nanoparticles and constituents of more complex mechanically interlocked systems, as well.

Self-assembling

It can be assumed that structurally different subunits induce various non-covalent interactions, whose overall effect directs the self-ordering of the synthesized compounds. The presence of fullerene substructure favors the hydrophobic and π–π interactions, the amide and carboxylic moieties regulate the organization driven by hydrogen bond formation, while aliphatic segments of amino acids moieties (GABA and Gly) support the hydrophobicity. Therefore, it could be expected that the fine tuning of intermolecular forces by structure changing would lead to different self-assembled forms.

The self-aggregation of fulleropeptides **2**–**12** was investigated by the SEM using their precursor Fp-GABA-OH **1** as a model compound and solid samples obtained by precipitation with methanol, as well as those deposited as a solution and allowed to dry by slow evaporation of the solvent at room temperature under toluene atmosphere [42]. Association of the model compound was examined in several individual solvents (*n*-hexane, dichloromethane, toluene, methanol) and their mixtures. The most ordered and uniformly distributed aggregates were obtained with PhMe/MeOH (5/1, v/v). Consequently, 11 remaining fulleropeptidic acids were investigated using their 1 mM solution in the same system. The SEM images of selected representatives are presented in Figs. 6 and 7 (solid samples and assembles obtained upon evaporation of the solvent, respectively) while the results of whole series of fulleropeptidic acids **2**–**12** are given in ESM.

The arrangement into micrometer sized needle-shaped forms (~ 3 μm long) with no further arrangement were observed after precipitation of the model compound, Fp-GABA-OH **1**, with polar protic solvent. Introduction of a peptide moiety provoked the change in the self-organization ability, with notable influence of the introduced chain structure (Fig. 6). Thus the homopeptides **2** and **3** formed attractive, hierarchically ordered flower-like aggregates, while the corresponding hetero di-and tripeptides **4**, **5**, and **7** organized into irregularly arranged needles or curled sheets. Further chain elongation up to pentapeptide led to the formation of well-arranged micrometer-sized flowers slightly varying in the petal thickness, while in the solid sample of the hexapeptide **12** low level of the self-organization was observed (Fig. 6 and ESM).

Obtained results indicate that even under quite extreme conditions, such as the fast aggregation, hierarchically ordered self-assembling could be achieved by alteration of the peptide subunit and consequent fine tuning of the hydrophobicity/hydrophilicity ratio. More detailed insight into the role of the peptide moiety in the arranging of fulleropeptides was obtained by the SEM analysis of aggregates formed after slow evaporation of the solvent (PhMe/MeOH 5/1, v/v). Generally, it was found that the fraction of more hydrophobic amino acid residue (i.e., GABA) in the whole molecule played important role in the self-ordering process (Fig. 7). Thus, compound **1** formed small dots-like structures which further grew into ellipsoidal flat plates ($\sim 1.3 \times 2$ μm). Both homo- and heterodipeptides **2** and **4**, as well as other peptides containing GABA-fragment (**5** and **6**) arranged into regular rods and further grew into radial, uniformly distributed flowers. Compounds containing $GABA_2$-fragment (**7**–**9**) initially formed dots which grew into curled sheets (some of them via regular circles), while in the presence of the $GABA_3$-subunit corresponding compounds (**3**, **10**–**12**) underwent higher level of hierarchical arrangement following the sequence dots—curled sheets—flowers (Fig. 7 and ESM). As can be seen, all fulleropeptides formed ordered 3D assemblies. Owing highly accessible surface area those structures could play a role in the development of new nanostructured materials with upgraded properties, applicable in diverse fields (catalysis, coating, bioactivity, etc).

In order to examine substrate effect on morphological features, samples of the pentapeptide **11**, prepared from PhMe/MeOH (5/1, v/v) solution by 'drop drying' method [12] were deposited on Si wafer, Al foil, and glass plate. Their SEM images, presented in Fig. 8 revealed that used compound assembled in the similar mode on Si and Al giving curled leafs, had further grown into hierarchically organized micrometer-sized flower-like particles (up to ~ 7 μm). Although the self-assemblies similar in shape and size were observed on both surfaces, the level of their hierarchical organization differed markedly. Thus, much more organized flower-like aggregates were built on silicon

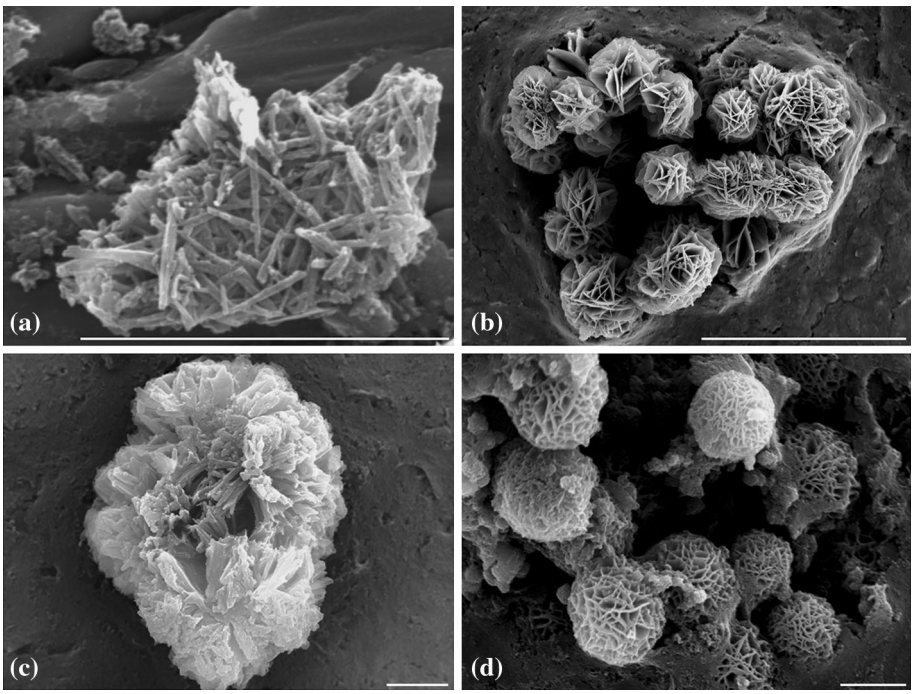

Fig. 6 SEM images of selected fulleropeptides representing an influence of the peptide chain on self-organization: model compound **1** (**a**), homodipeptide **2** (**b**), heterotripeptide **7** (**c**), and tetrapeptide **6** (**d**) deposited as methanolic precipitates on a brass substrate. Presented scale bars correspond to 10 μm

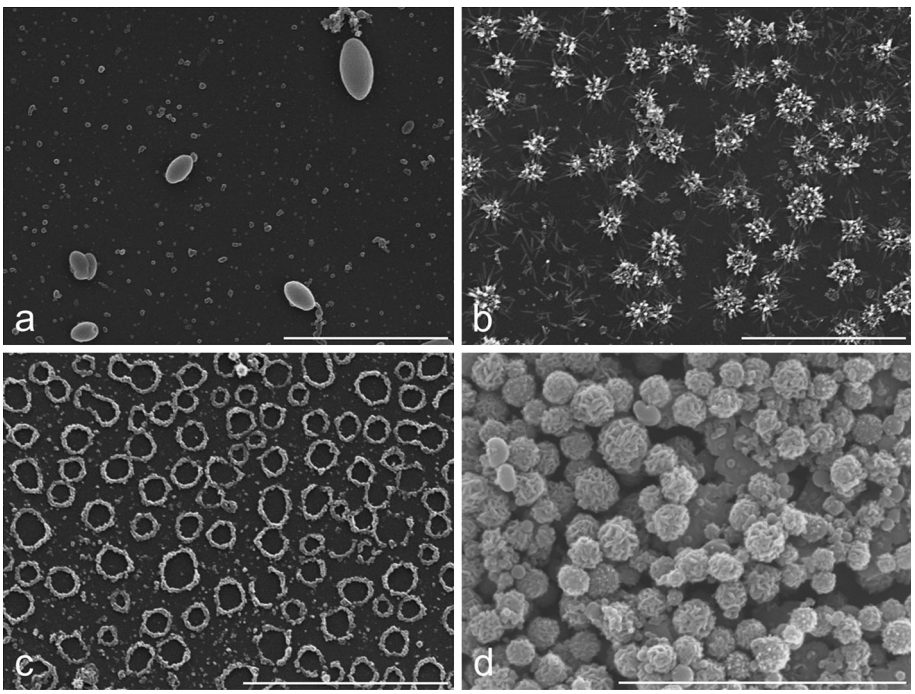

Fig. 7 SEM images of selected fulleropeptides representing an influence of the GABA-subunit on self-organization: model compound **1** (**a**), Fp-GABA-Gly-OH **4** (**b**), Fp-$GABA_2$-Gly-OH **7** (**c**), and Fp-$GABA_3$-OH **3** (**d**) prepared from PhMe/MeOH (5/1, v/v) on a Si substrate. Presented scale bars correspond to 10 μm

in comparison to aluminum surface (Fig. 8a, b, respectively). Deposition on a glass substrate afforded quite different uniformly distributed round particles of ~200 nm in diameter with low level of further arrangement (Fig. 8c). Obtained results indicate that interactions with metallic surfaces could play the role in the hierarchical self-organization of studied compound.

Antioxidant activity in vitro

The comparative evaluation of the antioxidant capacity of 12 fullerene acids and the parent fullerene was performed with their water soluble fullerosomal form with soybean lecithin, employing the FOX antioxidant assay [41, 43]. Briefly, to an aqueous solution of TBHP and fullerosome

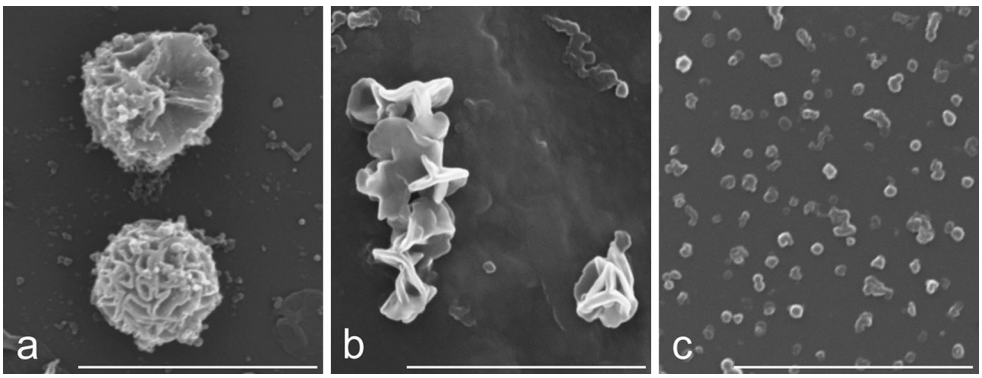

Fig. 8 SEM images of Fp-$(GABA)_3$-$(Gly)_2$-OH **11** after evaporation from PhMe/MeOH 5/1 mixture on Si wafer (**a**), Al foil (**b**), and glass (**c**). Presented scale bars correspond to 6 μm

the FOX reagent was added and the concentration of obtained colored complex was determined spectrophotometrically at 560 nm. Vitamin C was used as a positive control, while blank probe contained pure water instead of tested compounds. The compounds capacity to reduce the concentration of TBHP relative to equimolar quantity of vitamin C is presented in Table 1, and a detailed explanation is given in ESM.

Obtained results showed that all compounds expressed much better, 6–eight-fold higher radical scavenging activity than the control compound, vitamin C. At the same time the main part of fullerene acids **1–12** achieved even slightly better antioxidant capacity than non-functionalized fullerene C_{60}. It could be supposed that introduction of the peptide chain led to improved solubility of synthesized derivatives, and consequently to the suppression of their aggregation. Thus, being more available to the approaching hydroperoxide, compounds expressed better radical scavenging ability. As mentioned before, formation of homogenous three dimensional supramolecular clusters with enhanced surface-to-volume-ratio led to the improvement of the antioxidant activity.

Table 1 The antioxidant capacity (A_{ox}) of fullerene acids **1–12** and C_{60} relative to vitamin C

Compound	A_{ox} vs vitamin C
1	7.3
2	8.2
3	8.1
4	6.3
5	7.8
6	8.2
7	5.6
8	5.5
9	8.4
10	6.2
11	7.4
12	9.6
C_{60}	5.8
Vitamin C	1.0

Electrochemical properties

The electrochemical properties of fulleropeptides **2–12** and their precursor Fp-GABA-OH **1** were examined by cyclic voltammetry at the room temperature using 1 mM solution of tested compound in DMF in the presence of TBAP as supporting electrolyte, Fc/Fc^+ couple as an internal standard, and a glassy carbon electrode. The cyclic voltammogram of the chosen representative **12** is depicted in the Fig. 9, while the CV curves of all other fulleroacids **1–11** are given in ESM. In the applied potential window, all compounds gave four well-separated waves attributable to consecutive one-electron, fullerene-centered reductions. Besides expected cathodic shift due to carbon core functionalization (~0.2 V in comparison to pristine C_{60}), introduction of the peptide fragment did not provoke significant change in electrochemical properties of

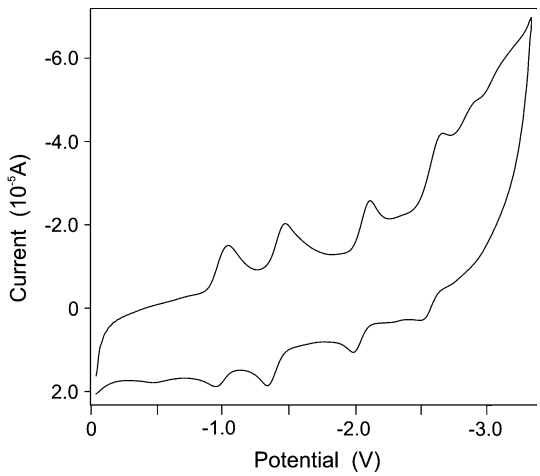

Fig. 9 Cyclic voltammogram of fulleropeptide acid **12**

Table 2 Half-wave reduction potentials of fullerene acids **1–12** vs. Fc/Fc^+, in DMF containing 0.1 M TBAP as the supporting electrolyte

Compound	$E_{1/2}$ (V)			
	I	II	III	IV
C_{60}[a]	−0.77	−1.25	−1.84	−2.38
1	−0.95	−1.40	−2.04	−2.58
2	−0.95	−1.39	−2.04	−2.58
3	−0.95	−1.40	−2.05	−2.60
4	−0.96	−1.39	−2.04	−2.58
5	−0.96	−1.41	−2.05	−2.60
6	−1.01	−1.42	−2.07	−2.60
7	−0.96	−1.39	−2.04	−2.58
8	−0.96	−1.40	−2.03	−2.58
9	−1.00	−1.40	−2.04	−2.58
10	−0.96	−1.39	−2.03	−2.57
11	−0.97	−1.41	−2.05	−2.57
12	−0.99	−1.40	−2.05	−2.58

[a] The literature data [44] are recalculated to the Fc/Fc^+ value

fulleropeptides (Table 2). Thus, half-wave potentials of all four reductions, found at approximately −1, −1.4, −2, and −2.6 V appeared in narrow range along whole series of fulleropeptides **2–12** and did not differ much from the model compound **1**. Nevertheless, a slightly impeded first reduction (for ∼50 mV) was observed in compounds **6**, **9,** and **12** containing the Gly_3-fragment, that might be a consequence of the long-range electron-accepting effect of the closely distributed peptide functions.

Conclusions

A series of eleven new fullerene-peptide hybrids was synthesized and their structures were fully characterized by means of spectroscopic and spectrometric methods. The assignation of all spin active nuclei belonging to the peptide chain, done by comparative analysis of 1D and 2D NMR spectral data could facilitate further research and development of more complex fullerene-based peptidomimetics. Electrochemical properties of obtained compounds remained similar to non-functionalized fullerene C_{60}, with slightly attenuated electron-accepting ability particularly in compounds containing the Gly_3-subunit. Nevertheless, an introduction of the peptide backbone led to the improvement of solubility and aggregation suppression providing material with significant antioxidant activity. Also, morphology investigation revealed a relevant influence of the peptide side chain structure on compounds ordering. In contrast to solid sample of the model compound **1**, where fine needle-shaped forms without further organization were observed, the majority of fulleropeptides **2–12** underwent multi-stage hierarchical organization to regular, attractive flowers. Investigation of solvent-assisted organization of compounds provided a more detailed insight into the role of peptide fragment. A notable influence of the hydrophobic, i.e., GABA-segment on a regular, gradual organization of different forms was observed. In addition, non-covalent interactions with metallic surface affected the level of hierarchical ordering of studied compounds. It could be assumed that aggregation in polar environment, driven by π–π and hydrophobic interactions afforded initial discoid nanoparticles. Additional stabilization by methanol-mediated hydrogen bonds with peptide and carboxylic groups provoked gradual folding to larger curled sheets or rods, and finally to flower-shaped forms.

Acknowledgements This work was supported by the Ministry of Education, Science and Technological Development (Project No. 172002).

References

1. Montellano López A, Mateo-Alonso A, Prato M (2011) Materials chemistry of fullerene C_{60} derivatives. J Mater Chem 21:1305–1318
2. Martín N (2006) New challenges in fullerene chemistry. Chem Commun 20:2093–2104
3. Lai Y-Y, Cheng Y-J, Hsu C-S (2014) Applications of functional fullerene materials in polymer solar cells. Energy Environ Sci 7:1866–1883
4. Liu Y, Zhao J, Li Z, Mu C, Ma W, Hu H, Jiang K, Lin H, Ade H, Yan H (2014) Aggregation and morphology control enables multiple cases of high-efficiency polymer solar cells. Nat Commun 5:5293. doi:10.1038/ncomms6293
5. Yan W, Seifermann SM, Pierrat P, Bräse S (2015) Synthesis of highly functionalized C_{60} fullerene derivatives and their applications in material and life sciences. Org Biomol Chem 13:25–54
6. Bosi S, Da Ros T, Spalluto G, Prato M (2003) Fullerene derivatives: an attractive tool for biological applications. Eur J Med Chem 38:913–923
7. Bakry R, Vallant RM, Najam-ul-Haq M, Rainer M, Szabo Z, Huck CW, Bonn GK (2007) Medicinal applications of fullerenes. Int J Nanomed 2:639–649
8. Partha R, Conyers JL (2009) Biomedical applications of functionalized fullerene-based nanomaterials. Int J Nanomed 4:261–275
9. Bjelakovic MS, Godjevac DM, Milic DR (2007) Synthesis and antioxidant properties of fullero-steroidal covalent conjugates. Carbon 45:2260–2265
10. Diederich F, Gómez-López M (1999) Supramolecular fullerene chemistry. Chem Soc Rev 28:263–277
11. Zhang E-Y, Wang C-R (2009) Fullerene self-assembly and supramolecular nanostructures. Curr Opin Colloid Interface Sci 14:148–156
12. Babu SS, Möhwald H, Nakanishi T (2010) Recent progress in morphology control of supramolecular fullerene assemblies and its applications. Chem Soc Rev 39:4021–4035

13. Guldi DM, Zerbetto F, Georgakilas V, Prato M (2005) Ordering fullerene materials at nanometer dimensions. Acc Chem Res 38:38–43
14. Lens M (2009) Use of fullerenes in cosmetics. Recent Pat Biotechnol 3:118–123
15. Tam J, Liu J, Yao Z (2013) Effect of microstructure on the antioxidant properties of fullerene polymer solutions. RSC Adv 3:4622–4627
16. Nakanishi T (2010) Supramolecular soft and hard materials based on self-assembly algorithms of alkyl-conjugated fullerenes. Chem Commun 46:3425–3436
17. Asanuma H, Li H, Nakanishi T, Möhwald H (2010) Fullerene derivatives that bear aliphatic chains as unusual surfactants: hierarchical self-organization, diverse morphologies, and functions. Chem Eur J 16:9330–9338
18. Kawauchi T, Kumaki J, Yashima E (2006) Nanosphere and nanonetwork formations of [60]fullerene-end-capped stereoregular poly(methylmethacrylate)s through stereocomplex formation combined with self-assembly of the fullerenes. J Am Chem Soc 128:10560–10567
19. Gan H, Liu H, Li Y, Gan L, Jiang L, Jiu T, Wang N, He X, Zhu D (2005) Fabrication of fullerene nanotube arrays using a template technique. Carbon 43:205–208
20. Cassell AM, Asplund CL, Tour JM (1999) Self-assembling supramolecular nanostructures from a C_{60} derivative: nanorods and vesicles. Angew Chem Int Ed 38:2403–2405
21. Geng J, Zhou W, Skelton P, Yue W, Kinloch IA, Windle AH, Johnson BFG (2008) Crystal structure and growth mechanism of unusually long fullerene (C60) nanowires. J Am Chem Soc 130:2527–2534
22. Wang N, Li Y, He X, Gan H, Li Y, Huang C, Xu X, Xiao J, Wang S, Liu H, Zhu D (2006) Synthesis and characterization of a novel electrical and optical-active triads containing fullerene and perylenebisimide units. Tetrahedron 62:1216–1222
23. Prato M, Bianco A, Maggini M, Scorrano G, Toniolo C, Wudl F (1993) Synthesis and characterization of the first fullerene-peptide. J Org Chem 58:5578–5580
24. Bianco A, Bertolini T, Crizma M, Valle G, Toniolo C, Maggini M, Scorrano G, Prato M (1997) β-Turn induction by C_{60}-based fulleroproline: synthesis and conformational characterization of Fpr/Pro small peptides. J Pept Res 50:159–170
25. Sofou P, Elemes Y, Panou-Pomonis E, Stavrakoudis A, Tsikaris V, Sakarellos C, Sakarellos-Daitsiotis M, Maggini M, Formaggio F, Toniolo C (2004) Synthesis of a proline-rich [60]fullerene peptide with potential biological activity. Tetrahedron 60:2823–2828
26. Tsumoto H, Takahashi K, Suzuki T, Nakagawa H, Kohda K, Miyata N (2008) Preparation of C_{60}-based active esters and coupling of C_{60} moiety to amines or alcohols. Bioorg Med Chem Lett 18:657–660
27. Yang J, Alemany LB, Driver J, Hartgerink JD, Barron AR (2007) Fullerene-derivatized amino acids: synthesis, characterization, antioxidant properties, and solid-phase peptide synthesis. Chem Eur J 13:2530–2545
28. Bianco A (2005) Efficient solid-phase synthesis of fullero-peptides using merrifield strategy. Chem Commun 25:3174–3176
29. Aroua S, Schweizer WB, Yamakoshi Y (2014) C_{60} pyrrolidine bis-carboxylic acid derivative as a versatile precursor for biocompatible fullerenes. Org Lett 16:1688–1691
30. Toniolo C, Bianco A, Maggini M, Scorrano G, Prato M, Marastoni M, Tomatis R, Spisani S, Palú G, Blair ED (1994) A bioactive fullerene peptide. J Med Chem 37:4558–4562
31. Pantarotto D, Tagmatarchis N, Bianco A, Prato M (2004) Synthesis and biological properties of fullerene-containing amino acids and peptides. Mini Rev Med Chem 4:805–814
32. Rouse JG, Yang J, Ryman-Rasmussen JP, Barron AR, Monteiro-Riviere NA (2007) Effects of mechanical flexion on the penetration of fullerene amino acid-derivatized peptide nanoparticles through skin. Nano Lett 7:155–160
33. Yang J, Wang K, Driver J, Yang J, Barron AR (2007) The use of fullerene substituted phenylalanine amino acid as a passport for peptides through cell membranes. Org Biomol Chem 5:260–266
34. Jennepalli S, Pyne SG, Keller PA (2014) [60]Fullerenyl amino acids and peptides: a review of their synthesis and applications. RSC Adv 4:46383–46398
35. Sun T, Xu Z (2006) Radical scavenging activities of α-alanine C_{60} adduct. Bioorg Med Chem Lett 16:3731–3734
36. Gazit E (2007) Self-assembled peptide nanostructures: the design of molecular building blocks and their technological utilization. Chem Soc Rev 36:1263–1269
37. Belavtseva EM, Romanova VS, Lapshin AI, Kuleshova EF, Parnes ZN, Vol'pin ME (1996) Electron microscopy study of amino acid derivatives of [60]fullerene in non-aqueous solution. Mendeleev Commun 6:171–173
38. Vol'pin ME, Belavtseva EM, Romanova VS, Lapshin AI, Aref'eva LI, Parnes ZN (1995) Self-assembling of associates of amino acids and dipeptide derivatives of [60]fullerene in aqueous solution: a study by scanning electron microscopy. Mendeleev Commun 5:129–131
39. Bjelaković M, Todorović N, Milić D (2012) An approach to nanobioparticles—synthesis and characterization of novel fulleropeptides. Eur J Org Chem 2012:5291–5300
40. Bjelaković MS, Kop TJ, Vlajić M, Đorđević J, Milić DR (2014) Design, synthesis, and characterization of fullerene-peptide-steroid covalent hybrids. Tetrahedron 70:8564–8570
41. Lens MB, De Marni E, Gullo R, Citernesi U and Crippa R (2007) Liposomes loaded with fullerene and process for their preparation, WO, 2007043074
42. Zhang X, Takeuchi M (2009) Controlled fabrication of fullerene C_{60} into microspheres of nanoplates through porphyrin-polymer-assisted self-assembly. Angew Chem Int Ed 48:9646–9651
43. Bou R, Codony R, Tres A, Decker EA, Guardiola F (2008) Determination of hydroperoxides in foods and biological samples by the ferrous oxidation-xylenol orange method: a review of the factors that influence the method's performance. Anal Biochem 377:1–15
44. Dubois D, Moninot G, Kutner W, Jones MT, Kadish KM (1992) Electroreduction of buckminsterfullerene, C_{60}, in aprotic solvents Solvent, supporting electrolyte, and temperature effects. J Phys Chem 96:7137–7145